Acta Crystallographica Section D
Biological Crystallography
ISSN 0907-4449

Active-site changes in the pyruvate dehydrogenase multienzyme complex E1 apoenzyme component from *Escherichia coli* observed at 2.32 Å resolution

Krishnamoorthy Chandrasekhar,[a,b]‡ Palaniappa Arjunan,[a,b]‡ Martin Sax,[a] Natalia Nemeria,[c] Frank Jordan[c] and William Furey[a,b]*

[a]Biocrystallography Laboratory, Veterans Affairs Medical Center, PO Box 12055, University Drive C, Pittsburgh, PA 15240, USA, [b]Department of Pharmacology, University of Pittsburgh School of Medicine, 1340 BSTWR, Pittsburgh, PA 15261, USA, and [c]Department of Chemistry, Rutgers University, Newark, NJ 07102, USA

‡ These authors contributed equally to the success of this study.

Correspondence e-mail: fureyw@pitt.edu

Received 24 July 2006
Accepted 27 August 2006

PDB Reference: pyruvate dehydrogenase E1 component, 2g67, r2g67sf.

The first enzymatic component, E1 (EC 1.2.4.1), of the pyruvate dehydrogenase multienzyme complex (PDHc) utilizes thiamine diphosphate (ThDP) and Mg^{2+} as cofactors. The structure of a branched-chain-specific E1 apoenzyme from the heterotetrameric $\alpha_2\beta_2$ E1 family was recently reported and showed that disorder-to-order transformations in two active-site loops take place upon cofactor binding. To ascertain what effect the absence of cofactor may have in the homodimeric α_2 *Escherichia coli* PDHc E1, the corresponding apoenzyme has been prepared and its three-dimensional structure determined and analyzed at 2.32 Å by crystallographic methods. This represents the first reported apoenzyme structure for any E1 component from the homodimeric α_2 family. Electron-density features occurring in the region where the cofactor pyrimidine ring would normally be expected to bind are of size, shape and location compatible with water molecules that form a hydrogen-bonded linkage between residues Glu571 and Val192, which normally make conserved interactions with the ThDP cofactor. A histidine side chain that normally forms hydrogen bonds to ThDP is disordered in its absence and partially occupies two sites. Unlike in the reported heterotetrameric branched-chain apo-E1, no disorder/order loop transformations are evident in apo-PDHc E1 relative to the holo-E1 enzyme (PDHc E1–ThDP–Mg^{2+}). Differences in the extent of hydrogen-bonding networks found in the apo-E1 enzyme, the holo-E1 enzyme and in an inhibitor complex with bound thiamine 2-thiazolone diphosphate (ThTDP), PDHc E1–ThTDP–Mg^{2+}, are described.

1. Introduction

The *Escherichia coli* pyruvate dehydrogenase multienzyme complex (PDHc; Reed, 1974) catalyzes the oxidative decarboxylation of pyruvate,

$$\text{pyruvate} + \text{coenzyme A} + \text{NAD}^+ \longrightarrow \text{acetyl-coenzyme A} + \text{CO}_2 + \text{NADH} + \text{H}^+.$$

The pyruvate dehydrogenase complex is one of the most studied members and is arguably the most important member of the family of 2-oxoacid dehydrogenase multienzyme complexes. One enzymatic component of this complex, PDHc E1, catalyzes the first step of a multistep process using thiamine diphosphate (ThDP) and Mg^{2+} as cofactors. The E1 component from Gram-negative bacteria is a homodimer (α_2), while that from eukaryotes and many Gram-positive bacteria is a heterotetramer ($\alpha_2\beta_2$). Replacing the proton on C2 of ThDP by an O atom as in thiamine 2-thiazolone diphosphate (ThTDP) or by an S atom as in thiamine 2-thiothiazolone diphosphate (ThTTDP) inactivates the enzyme. Structural

features and solvent-mediated hydrogen-bonding interactions explaining the substantially larger binding affinity to the enzyme of ThTDP than ThDP have been discussed and mechanistic roles for structural reorganization and reversal in PDHc E1 have been presented (Arjunan *et al.*, 2004). In the crystal structures of the ThDP (holo-E1) and ThTDP complexes, two identical subunits of 886 amino acids form dimers. The ThDP or ThTDP molecules are located at the dimer interfaces, with residues from both subunits contributing to their binding. In the recently reported crystal structure of a branched-chain-specific E1 apoenzyme from the heterotetrameric $\alpha_2\beta_2$ family, it was found that the absence of cofactor resulted in an order-to-disorder transformation of two loops near the active site (Nakai *et al.*, 2004). In the corresponding branched-chain E1 holoenzyme these loops were found to close in on and cover most of the cofactor, shielding it from solvent. It is of interest to determine whether this is a general effect important for all ThDP-dependent enzymes and imposes additional stability or whether it is specific to the heterotetrameric E1 enzyme family. To probe the issue, the crystal structure of the homodimeric *E. coli* PDHc E1 apoenzyme (sansThDP and Mg^{2+}) has now been determined at 2.32 Å and is compared with the structures of the corresponding ThTDP complex (Arjunan *et al.*, 2004) and holo-E1 enzyme (Arjunan *et al.*, 2002), as well as with the branched-chain heterotetrameric E1 apoenzyme (Nakai *et al.*, 2004).

2. Experimental

PDHc E1 from *E. coli* was purified and assayed according to the procedures of Nemeria *et al.* (2001) and McNally *et al.* (1995). The enzyme was overexpressed from the pGS878 plasmid (JRG3304) and any ThDP or Mg^{2+} present was removed by gel filtration using a G-25 column. The column was equilibrated with 20 m*M* HEPES buffer pH 7.0 containing 5 m*M* dithiothreitol (DTT), 0.2% NaN_3, 0.5 m*M* ethylenediamine tetraacetate (EDTA) and 1 µ*M* leupeptin. Specific activity measurements indicated that the resulting enzyme was indeed inactive. The apoenzyme was crystallized by the sitting-drop vapour-diffusion method, mixing equal amounts of protein and precipitant solutions. The best crystals were obtained with a reservoir solution containing 15–20% PEG 2000 monomethyl ether, 5–10% 2-propanol, 0.2% NaN_3 and 100 m*M* HEPES buffer pH 7.05 at 295 K. Crystals grew in four to five weeks and were typically of approximate dimensions $0.3 \times 0.2 \times 0.1$ mm.

A low-temperature (93 K) data set was collected from a single crystal with a Bruker HiStar multiwire area detector on a Rigaku RU-200 rotating-anode generator operating at 42 kV and 65 mA. The focal spot was 0.2×2.0 mm and Osmic mirrors were used to provide a highly focused beam. Data were processed using *XGEN* (Howard *et al.*, 1987) through the calculation of integrated intensities and then scaled and reduced to a set of unique intensities with locally modified programs of Weisman (1982). The crystal diffracted to 2.32 Å; the Matthews coefficient V_M was evaluated to be 2.30 Å^3 Da^{-1} based on one dimer per asymmetric unit.

Table 1
Crystallographic data and refinement statistics.

Values in parentheses are for the last shell.

Data statistics	
Space group	$P2_1$
Unit-cell parameters (Å, °)	$a = 81.61$, $b = 140.63$, $c = 81.91$, $\beta = 102.87$
Diffraction limit (Å)	2.32
Completeness (%)	91.7 (44.1)
Total No. of reflections	203875
No. of unique reflections	71362
R_{merge} (on I)	0.060
X-ray source	Rigaku RU200
Wavelength (Å)	1.5418
Refinement	
Resolution range (Å)	34.7–2.32
No. of reflections ($I > \sigma$)	70893
No. of reflections for test set	3588
R factor	0.212 (0.203)
R_{free}	0.281 (0.304)
No. of residues	1602
No. of protein atoms	12682
No. of solvent atoms	448
Average B factor (Å^2)	
All atoms	15.37
Protein atoms	15.39
Solvent atoms	14.79
Estimated coordinate error† (Å)	0.26
R.m.s. deviations	
Bond lengths (Å)	0.010
Bond angles (°)	1.546

† From a Luzzati plot (Luzzati, 1952).

The apo-PDHC E1 crystals are isomorphous to those of the ThDP and ThTDP complexes, crystallizing in the same space group $P2_1$ with unit-cell parameters that differ by less than 0.5%. The structure of the apoenzyme was therefore determined starting with the final refined coordinates of the ThDP complex, omitting ThDP, Mg^{2+}, solvent molecules and protein residues in the immediate vicinity of the active-site region. Following rigid-body refinement, simulated annealing was performed with the *CNS* program (Brünger *et al.*, 1998) and a $(2F_o - F_c)$ composite OMIT map was calculated in which approximately 2–5% of the structure was omitted in stages. The map revealed the locations of the omitted active-site residues, but no clear electron density was seen to indicate the presence of the cofactors ThDP or Mg^{2+}. The composite OMIT map was examined carefully using the graphics program *O* (Jones *et al.*, 1991) and adjustments of residues were made wherever necessary. Interestingly, in both molecules in the asymmetric unit strong electron density clearly indicated that His142, a residue in the active site, was disordered, partially occupying two rotomer conformations. The alternate conformation setup procedure in *CNS* was followed to provide for this 'disordered' feature of His142. The occupancies of both sites for this residue were refined, followed by positional refinement of the structure. This tandem procedure was repeated several times and the $(2F_o - F_c)$ and $(F_o - F_c)$ maps were examined again to look for signs of the cofactors. The primary electron density visible constituted two globules, indicating the presence of water molecules, in the region

where the pyrimidine ring would be expected to bind. 448 solvent molecules were positioned using *CNS* and examined using *O* and final positional minimization of the structure was performed followed by group and individual *B*-factor refinements. Crystallographic data and final refinement statistics are detailed in Table 1.

3. Results

The crystal structure of apo-PDHc E1 is similar to the previously reported structures of the ThDP and ThTDP complexes. The root-mean-square deviation for corresponding protein C^{α} atoms is 0.18 Å between the ThDP and ThTDP complexes, 0.36 Å between the ThDP complex and apo-PDHc E1 and 0.39 Å between the ThTDP complex and apo-PDHc E1. However, for residues in the vicinity of the active site alone, these deviations increase to approximately 0.45 Å between the ThDP or ThTDP complex and apo-PDHc E1. The slightly lower (by $\sim$0.6 Å^2) *B* values for solvent atoms relative to protein is likely to be near the standard deviation for that quantity and thus is not significant, but may also reflect the fact that only tightly bound and clearly identifiable water molecules were included in the model. Hydrogen-bonding interactions in the ThDP- and ThTDP-binding regions of the respective complexes have been analyzed in detail and the role of solvent in enzyme inhibition and catalysis has been discussed (Arjunan *et al.*, 2004). Many of the water molecules found in the apoenzyme structure occur in virtually the same positions as in the other two structures, giving rise in general to the same hydrogen-bonding interactions. However, there are, as expected, some significant differences in the vicinity of the cofactor-binding site, as can be seen from Figs. 1 and 2. Considering the 25 residues in each monomer immediately surrounding the region, there are 72 solvent molecules in the ThTDP complex structure, 65 in the ThDP complex structure and 37 in the apo-PDHc E1 structure within 3.5 Å of any of these residues, suggesting a gradual relaxation of hydrogen-bond stabilizing interactions from inhibited PDHc E1 to the coenzyme-bound form to apo-PDHc E1. In order to ensure that these results are not just artifacts of resolution-limit differences between the three structures (1.85 Å for the ThDP complex, 2.1 Å for the ThTDP complex and 2.32 Å for apo-PDHc E1), the ThDP and ThTDP complex structures were reanalyzed, omitting all solvent molecules, performing the entire set of refinement procedures again with data truncated to 2.32 Å and subsequently identifying solvent molecules by evaluating $(F_o - F_c)$ maps. In the ThDP complex, all 65 solvent atoms mentioned were found at electron-density values of $\geq 2\sigma$, with all but three at $\geq 3\sigma$. In the ThTDP complex, all 72 solvent atoms were found at $\geq 2\sigma$, with all but eight at $\geq 3\sigma$. Further, using scaled observed data sets only, maps with $(F_{holo} - F_{apo})$ and $(F_{inhibited} - F_{apo})$ coefficients were calculated, phased with unbiased coordinates devoid of solvent atoms. In each of these maps, in the active-site region discussed earlier nearly twice the number of peaks were found with positive density values than with negative density values of the same magnitude [for example, at density values 3.5 times the σ level, 56 positive and 28 negative peaks were found in the $(F_{holo} - F_{apo})$ map and 94 positive and 53 negative peaks in the $(F_{inhibited} - F_{apo})$ map]. In the light of the above analyses, the presence of more numerous solvent molecules and hydrogen-bonded interactions in the ThTDP complex and ThDP complex compared with the apo-PDHc E1 enzyme is a real feature and cannot simply be attributed to different data-set resolutions.

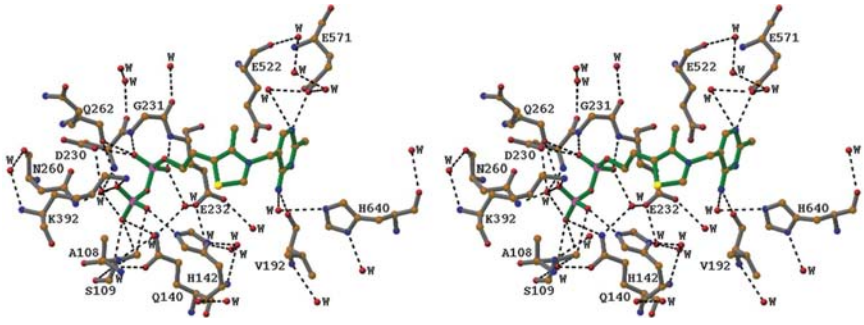

Figure 1
Stereodiagram of the holo-E1 enzyme from *E. coli* PDHc showing hydrogen bonds in the region around ThDP. The coordination of Mg^{2+} in the active site is not shown. This figure was prepared with the program *RIBBONS* (Carson, 1991).

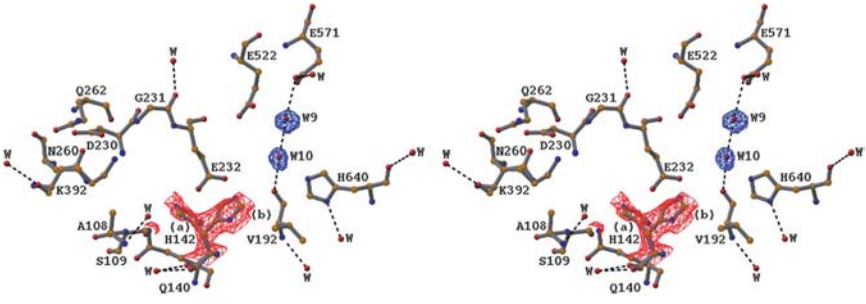

Figure 2
Stereodiagram of apo-PDHc E1 from *E. coli* showing hydrogen bonds in the same region as shown for holo-E1 in Fig. 1. Electron density in a $(2F_o - F_c)$ map indicating dual disordered positions of His142 is shown in red (contours at the 1.2σ level) and in an $(F_o - F_c)$ map indicating water-molecule assignments W9 and W10 in blue (contours at the 3.2σ level). This figure was prepared with the program *RIBBONS* (Carson, 1991).

Water molecules W4 found only in the ThDP complex, W6 and W7 found only in the ThTDP complex and W3 found in both are all absent in apo-PDHc E1. This is quite logical: in the former W4 links the cofactor ThDP and protein through hydrogen bonds with the N4′ atom and His640 NE2 and in the latter W6 and W7 contribute to an intricate hydrogen-bonding network connecting the inhibitor and protein; in both complexes W3 forms hydrogen bonds with O13 and Gln140 NE2 and in the ThTDP complex it also takes part in a hydrogen

bond involving Met194 SD. In the absence of cofactor or inhibitor, it could be expected that some water molecules vital to linking either of them with the protein would not be present. W8, which is present in the ThTDP complex, forming hydrogen bonds with Gly105 N, His106 NE2 and Glu636 OE2, but is not found in the ThDP complex, is observed in apo-PDHc E1 and is involved in the same interactions. The hydrogen bond between Arg263 O and Lys392 NZ of the same subunit is observed only in the ThTDP complex (∼2.7 Å) and is absent in both the ThDP complex (∼3.75 Å) and apo-PDHc E1 (∼4.3 Å).

At no stage of the structure determination or refinement procedure was clear electron density visible for ThDP in either a $(2F_o - F_c)$ or an $(F_o - F_c)$ Fourier map. Both maps showed isolated electron-density spheres in the region where the pyrimidine ring of the cofactor would be located if present and revealed no evidence for any other part of the cofactor. No density was found at all for the Mg^{2+} ion and this leads us to infer that the cofactors had indeed been successfully removed from the protein. The isolated density observed was accounted for by two water molecules, W9 and W10, unique to the apoenzyme, leading to a hydrogen-bond network consisting of Glu571 OE2–W9–W10–Val192 O. While in both the ThDP complex and ThTDP complex the linking between Val192 O of one subunit and Glu571 OE2 of the other occurs through the N4′ and N1′ atoms of the cofactor ThDP or inhibitor ThTDP, these two water molecules take on the role of the missing pyrimidine-ring atoms in the apoenzyme.

Regarding the two alternative conformations of His142, one of them was the same as that observed in the ThDP complex and ThTDP complex. These conformations refined to final occupancies of 0.36 and 0.64, the latter value being for the new position found only in apo-PDHc E1. An immediate consequence of this feature is the stereochemical hindrance that would occur between the histidine ring and the thiazolium ring of the cofactor, if the latter were indeed present. Conformational differences in the region of the active site of the enzyme between apo-PDHc E1, the ThDP complex and the ThTDP complex structures are shown in Fig. 3.

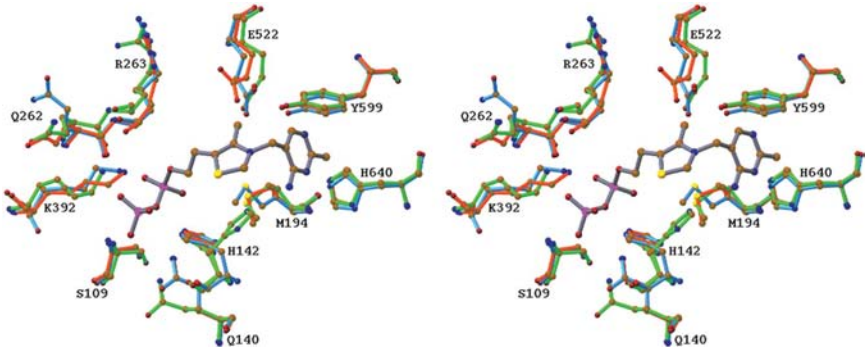

Figure 3
Stereodiagram superposing the holo-E1, the inhibited ThTDP complex and the apo-E1 structures of *E. coli* PDHc E1 based on least-squares alignment of all known C^{α} atoms. Residues in the holo-E1 structure are shown with blue bonds, those in the inhibited ThTDP structure with red bonds and those in the apo-E1 structure with green bonds. The ThDP molecule associated with the holo-E1 structure is shown in gray. This figure was prepared with the program *RIBBONS* (Carson, 1991).

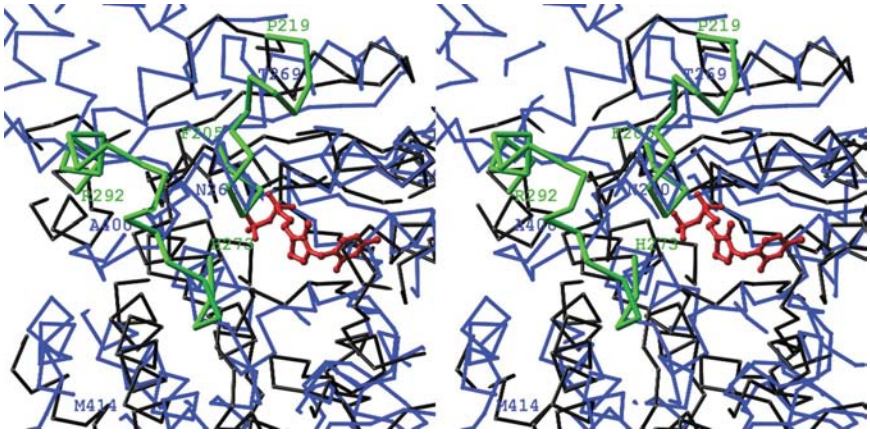

Figure 4
C^{α}-trace stereodiagram superposing the apo-E1 and holo-OXD structures based on least-squares alignment of the corresponding ThDP molecules associated with holo-E1 and holo-OXD. The backbone tertiary structures of holo-OXD and apo-OXD are essentially identical, as are those of holo-E1 and apo-E1. Residues in apo-E1 are shown in blue. Residues ordered in both holo-OXD and apo-OXD are shown in black and those ordered in holo-OXD but disordered in apo-OXD in green. The ThDP molecule associated with holo-OXD is shown in red. This figure was prepared with the program *RIBBONS* (Carson, 1991).

4. Discussion

It has been reported that binding of the cofactor ThDP to apo-transketolase (Sundström *et al.*, 1992) from *Saccharomyces cerevisae* and to the $\alpha_2\beta_2$ heterotetrameric E1 component of the branched chain 2-oxoacid dehydrogenase (OXD; Nakai *et al.*, 2004) from *Thermus thermophilus* HB8 induces a disorder–order transition in two loops adjacent to the active site. One of these loops, which directly participates in the binding of the cofactor, comprises the region Asn187–Ser198 in transketolase (TK) and Tyr206–Ser218 in OXD. This loop is flexible in both of these enzymes in the absence of the cofactor and only becomes ordered when the cofactor binds. In contrast, the corresponding loop residues Asn260–Thr269 in *E. coli* PDHc E1 show no disorder in the apoenzyme and adopt essentially the same conformation as in the corresponding holo-E1 enzyme. A second flexible loop occurs in the region Leu383–Glu393 in apo-transketolase. This corresponds to Glu522–Gln534 in PDHc E1 and Val37–Lys47 of the β-chain in OXD, both of which exhibit no disordered feature in any form of the respective enzymes studied. The loop Ser274–Trp291 of the α-chain in OXD that has uninterpretable electron density in the apoenzyme has no clear equivalence in

TK or PDHc E1. The loops Glu401–Asn413 and Asn541–Lys557 that are disordered in the PDHc E1 apoenzyme are also disordered in the holo-E1 enzyme as well as in the ThTDP complex. This disorder cannot therefore be attributed to the lack of coenzyme binding. It seems then that the disorder–order transition attributed to the binding of the cofactor ThDP is quite variable in PDHc E1, TK and OXD and neither involves equivalently positioned loops nor similar conditions for resuming order in all ThDP-dependent enzymes. The disordered regions in OXD are compared with those in apo-PDHc E1 in Fig. 4.

It appears reasonable to assume that the cofactor ThDP or inhibitor ThTDP aids in holding the PDHc E1 dimer together since it is located at an interface between the subunits and occurs twice in each functional dimer. The diphosphate end of the molecule forms hydrogen bonds to one subunit, while at the other end the aminopyrimidine moiety cross-links both subunits through hydrogen-bonding, ring-stacking and other weak intermolecular interactions. Thus, the bridging ThDP molecule helps to strengthen the bonding between subunits, but its removal does not change the mode of dimerization, as is demonstrated by the isomorphism of the crystal structures of the ThDP complex and apo-PDHc E1. Nevertheless, removal of the cofactor produces changes in the structure of the enzyme which are localized to regions close to the vacated binding site. Primarily, a significant reduction occurs in the number of bound or ordered water molecules and a positionally disordered histidine side chain is created. Evidently, the structural order near the vacated binding site diminishes. This contrasts with the changes that occur in this region of the protein when the inhibitor ThTDP replaces ThDP. In that case, the number of ordered water molecules is increased by the replacement, in turn leading to a more elaborate hydrogen-bonding network in this region in the inhibitor complex. The affinity of the protein is greater for the inhibitor than for the cofactor and the extensiveness of the hydrogen-bonding system seems to be a good qualitative measure of the tightness of binding in the complex (Arjunan *et al.*, 2004). Extending this interpretation to include α_2 apo-E1 implies that the complexes bind more tightly and perhaps increase in stability in the order apo-E1 < holo-E1 < inhibited E1.

This work was supported at Pittsburgh by the VA Merit Review Program and by NIH-GM-61791 (to WF) and at Rutgers by NIH-GM-62330 (to FJ).

References

Arjunan, P., Chandrasekhar, K., Sax, M., Brunskill, A., Nemeria, N., Jordan, F. & Furey, W. (2004). *Biochemistry*, **43**, 2405–2411.
Arjunan, P., Nemeria, N., Brunskill, A., Chandrasekhar, K., Sax, M., Yan, Y., Jordan, F., Guest, J. R. & Furey, W. (2002). *Biochemistry*, **41**, 5213–5221.
Brünger, A. T, Adams, P. D., Clore, G. M., DeLano, W. L., Gros, P., Grosse-Kunstleve, R. W., Jiang, J.-S., Kuszewski, J., Nilges, M., Pannu, N. S., Read, R. J., Rice, L. M., Simonson, T. & Warren, G. L. (1998). *Acta Cryst.* D**54**, 905–921.
Carson, M. (1991). *J. Appl. Cryst.* **24**, 958–961.
Howard, A. J., Gilliland, G. L., Finzel, B. C. & Poulos, T. L. (1987). *J. Appl. Cryst.* **20**, 383–387.
Jones, T. A., Zou, J.-Y., Cowan, S. W. & Kjeldgaard, M. (1991). *Acta Cryst.* A**47**, 110–119.
Luzzati, V. (1952). *Acta Cryst.* **5**, 802–810.
McNally, A. J., Motter, K. & Jordan, F. (1995). *J. Biol. Chem.* **270**, 19736–19743.
Nakai, T., Nakagawa, N., Maoka, N., Masui, R., Kuramitsu, S. & Kamiya, N. (2004). *J. Mol. Biol.* **337**, 1011–1033.
Nemeria, N., Yan, Y., Zhang, Z., Brown, A. M., Arjunan, P., Furey, W., Guest, J. R. & Jordan, F. (2001). *J. Biol. Chem.* **276**, 45969–45978.
Reed, L. J. (1974). *Acc. Chem. Res.* **7**, 40–46.
Sundström, M., Lindqvist, Y. & Schneider, G. (1992). *FEBS Lett.* **313**, 229–231.
Weisman, L. (1982). *Computational Crystallography*, edited by D. Sayre, pp. 56–63. Oxford: Clarendon Press.